Formaldehyde sensing by Co_3O_4 hollow spheres at room temperature

Yang Cao [a*], Jingyu Qian[b], Yong Yang [c], Yongguang Tu [d]

a Department of Energy and Resources Engineering, College of Engineering, Peking University, Beijing, 100871 P. R. China

b State Key Laboratory of Supramolecular Structure and Materials, College of Chemistry, Jilin University, 2699 Qianjin Street, Changchun 130012, China

c State Key Laboratory of Solidification Processing Center of Advanced Lubrication and Seal Materials, Northwestern Polytechnical University, Xi'an, Shaanxi 710072, P. R. China

d State Key Laboratory for Artificial Microstructure and Mesoscopic Physics, Department of Physics, Peking University, Beijing 100871, China.

*Corresponding author. Tel: +86-10- 62766853

E-mail address: caoyangchem@pku.edu.cn (Yang Cao).

Abstract: Formaldehyde is a ubiquitous and high toxicity gas. It is an essential task to efficient detect owing to their toxicity and diffusion. In this work, we studied on the detection of trace amount of formaldehyde based on hollow Co_3O_4 nanostructure. It is found that Co_3O_4 hollow spheres with different structures shows distinct sensing performance towards formaldehyde at room temperature, the response value of nanosheet modified Co_3O_4 towards 100 ppm formaldehyde will reach 35 in 18 second, and the nanoparticle modified Co_3O_4 hollow sphere will reach 2.1 in 18 second, 17 in 300 second. The nanosheet modified and nanoparticle modified Co_3O_4 hollow sphere will reach 4 and 20 in 10 second towards 100 ppm formaldehyde at room temperature. As room temperature, the sensors do not response towards NH_3, CO, etc. The sensing mechanism was proposed based on the theoretical and experimental results. The Co_3O_4 sensor shows that potential utility in CH_2O quick sensing at room temperature.

Keywords: Co_3O_4; formaldehyde sensing; room temperature; gas sensor; adsorption; theoretical results

1. Introduction

Aldehyde is a high toxic organic vapor and carcinogenic substance, which have been recognized as air pollutants by U.S. Environmental Protection Agency. [1] Aldehyde can be found in the surrounding air of polluted zones as well as most cities. [2] And more seriously is that aldehyde keep existence in indoor and do durative harm to humans. [3]

Until now, much work has been done about sensing for aldehyde, various method has been applied to detect formaldehyde, such as fluorescent method, [4] sophisticated optical methods, [5] gas chromatography, [6] quartz crystal microbalance sensor [7] and gas sensor. [8] Sensing of aldehyde by gas sensor has its advantage for the low price and easy operation. SnO_2,[9] ZnO,[10] TiO_2,[11] In_2O_3,[12] WO_3[13] have been studied for sensing of formaldehyde. The structure of the sensing material shows great influence to the sensing performance of the gas sensor. According to the numerous studies, large surface area and porosity can enhance the sensing performance. [14, 15] But there is still not much work on selective gas detection both on experiment work or theoretical work.

Co_3O_4, a p-type semiconductor with the direct band gap of 2.06 eV, [16] shows significant performance in catalysis, [17, 18] energy storage, [19] water splitting, [20] and gas sensing. [21] Especially, P-type semiconductor are promising materials for high-performance gas sensors. [22] Co_3O_4 have been used for sensing for ethanol, [23] NH_3, [24] NO_2, [25] CO. [26] In 2014, D. K. Lee and H. Song report on Co_3O_4 hollow sphere on sensing for aldehyde, and the sensing limit can reach 50 ppb at the

operation temperature of 220 ^{o}C. [27] Aihua Yuan et. al. synthesis the concave Co_3O_4 octahedral and the sensor's response are 3 for 1000 ppm formaldehyde at the operation temperature of 200 ^{o}C. [28] Mingzhe Zhang find that hollow nanotubes response towards 50 ppm aldehyde being 6.5 at 180 ^{o}C. [28]

In this work, we report the sensing ability of Co_3O_4 towards aldehyde at room temperature. The hollow sphere based Co_3O_4 nanostructure shows selective aldehyde response, and do not response to CO, acetone, NH_3, etc. We hypothesis that the sensing ability comes from the adsorption ability towards aldehyde gas molecule. The surface oxygen species and the surface nanosheet structure can enhance the sensing ability towards aldehyde.

2. Experimental

2.1 Chemicals and Reagents

Cobalt nitrate hexahydrate ($Co(NO_3)_2$•$6H_2O$) and glycerol were purchased from Sinopharm Chemical Reagent Corporation, isopropanol, ethanol, formaldehyde aqueous solution (37 %) were purchased from Beijing Chemical Works. All the above chemicals were used without any purification and distilled water were used in the experiment.

2.2 Synthesis of the Co_3O_4 hollow spheres

Cobalt glycerolate microsphere precursor were prepared by a solvothermal method described previously [31]. Typically, 8 mL glycerol (108.6 mmol) was dissolved in 30 mL isopropanol (391.8 mmol), a transparent solution can be formed under stirring for 1 h, then 0.3 g $Co(NO_3)_2$ (1.031 mmol) was added and

the mixture were stirred for 1 h to form a homogeneous and transparent solution. The solution was transferred into a 50 mL autoclave with Teflon-line. The autoclave was heated to 180 ^{o}C for 6 h. After the autoclave was cooled done to room temperature, the result precipitate was carefully collected and washed with absolute ethanol, then at 6000 rpm for 3 times. Finally, the precipitate was dried at 60 ^{o}C overnight.

Hollow cobalt oxide was synthesized by simply calcination of the cobalt glycerolate in the air at 350 ^{o}C, 450 ^{o}C, 550 ^{o}C, 650 ^{o}C, 750 ^{o}C with a heating rate at 1 ^{o}C/min.

Cobalt oxide nanosheet modified hollow spheres were synthesized by two steps according to the previous work. [31] Typically, 0.1 g cobalt glycerolate were dispersed in 20 mL distilled water. Then the mixture was transferred to a 50 mL autoclave with Teflon line. The autoclave was heated at 160 ^{o}C for 6 h to get cobalt hydroxide. The green cobalt hydroxide was washed with ethanol and dried at 60 ^{o}C overnight. Then calcite the cobalt hydroxide at 300 ^{o}C, 400 ^{o}C and 500 ^{o}C at a rate of 1 ^{o}C/min and hold for 2 h in the air atmosphere.

2.3 Characterization

The X-ray diffraction information of the materials were collected on a Rigaku D/MAX 2550 with Cu Kα anode (λ=1.5418 Å). The SEM, TEM and HRTEM images were taken on a JEOL JSM-6700F Scanning electron microscope and a FEI Tecnai G2 S-Twim F20 transmission electron microscope. The element composition and chemical state information of the materials were analysed by X-ray photoelectron

spectroscopy on a Thermo Fisher Escalab 250. N_2 adsorption/desorption isotherms test were performed on a Micromeritics ASAP 2020M system. The infrared spectra of the material were acquired by a Bruker IFS 66V/S FTIR spectrometer with KBr pellets of mixture of the sample and dry KBr powder fabricated by a press machine.

2.4 Sensor fabrication and testing

A commercially available alumina ceramic tube was used as substrate for testing the performance of the gas sensor. Two Au electrode connected with four Pt wires were attached on the surface of the alumina substrate. A certain amount of Co_3O_4 materials were dispersed in 1 mL ethanol to form a black slurry, then the slurry was put onto the surface of the alumina ceramic substrate. After ethanol were volatile into the air, the Co_3O_4 material were attached to the surface. Then a Ni-Cr alloy heating coil were carefully passed through the inner channel of the substrate to ensure the sensor could be heated at a setting power. The sensor was aged at 200 ^oC for 12 h to get good stability and then test on a CGS-8 Gas Sensing Measurement System (Beijing Elite Tech Company). The resistance of the sensor can be measured online by the sensing system. The sensing test were performed in a 1 L chamber of static gas system. Formaldehyde solution (37 %) were used to generate the formaldehyde gas vapour at different concentration. To ensure the gas concentration, the generated formaldehyde gas was kept at room temperature (25 ^oC) for about 2 hours to get balance before the test. The operation temperature was set at room temperature (25 ^oC). To ensure the results, the humidity was identical at 20 %

during the test. To help the gas molecules desorb from the surface of the sensor and sensor recover to beginning stage, a heating period of 30 second to a few minutes at 200 ^{o}C were applied.

2.5 Simulation and models

The setting of calculation model and relative parameters were chosen according to the literature. [31, 32]

The theoretical study uses the Vienna ab initio simulation package (VASP) to perform formaldehyde adsorption behavior on Co_3O_4 surface. And generalized gradient approximation (GGA) in the form of Perdew-Burke-Ernzerhof (PBE) was applied to the electronic structure.

The calculation for the adsorption of formaldehyde on the (110) plane were based on GGA+U method of VASP package. U-J= 5.0 eV were chosen to fit the experimental band gap.

3. Results and Discussion

3.1. Phase, Composition and morphology of cobalt glycerolate precursor

The typical SEM, TEM of cobalt glycerolate were shown in Fig. 3(A). As shown in Fig. 3(A), the cobalt glycerolate shows sphere like morphology. The spheres are around 300 nm. The X-ray diffraction patterns of the cobalt glycerolate sample was shown in Fig. 3(B), the only peak at about 10^{o} shows the low crystallization. The FT-IR spectra of the cobalt glycerolate were in Fig. S1 the supporting information.

3.2. Phase, Composition and morphology of cobalt oxide hollow spheres

The cobalt glycerolate were calcined in the air atmosphere to transfer into nanostructured Co_3O_4. Then the phase, composition and morphology of the cobalt oxide were examined. Fig. 4 shows the X-ray diffraction patterns of the cobalt oxide calcined at different temperature. The XRD pattern can be indexed to Co_3O_4 of cubic phase. And it shows better crystallization at the higher calcination temperature.

Fig. 5 shows the typical SEM images of the cobalt oxide spheres by calcite the cobalt glycerolate precursor in the region ranging from 350 ^oC to 750 ^oC. As it can be seen, when calcited at 350 ^oC, the surface of the Co_3O_4 keep the sphere morphology (Fig. 5A). And it shows small hole on the surface. When calcite the cobalt glycerolate at 650 ^oC, the sphere morphology changes, it shows nanoparticles on the surface of the material and holes can be seen clearly (Fig. 5D). When calcinate the cobalt glycerolate at 750 ^oC, it can be seen clearly that the material can hardly keep the sphere's morphology (Fig. 5E). The FT-IR spectroscopy of the Co_3O_4 were in Fig. S2 in supporting information. The O 1s and Co 2p XPS spectroscopy were shown in Fig. S3 and S4. The N_2 absorption isotherm spectroscopy were shown in Fig. S5. Fig. 6 shows typical TEM and HRTEM photo for the hollow Co_3O_4 calcite at 550 ^oC.

Fig. 7 shows the XRD pattern of the cobalt oxide hollow sphere modified with nanosheet calcite the $Co(OH)_2$ precursor at 300 ^oC, 400 ^oC, 500 ^oC. The diffraction peaks show that the materials are convert into Co_3O_4. (The XRD pattern of the $Co(OH)_2$ are shown in Fig. S6) It can be seen clearly the cobalt

oxide nanosheet in Fig. S7 that calcite at 300 ^{o}C hold the structure of the nanosheet. Fig. 8 shows the typical TEM and HRTEM images of the cobalt oxide spheres modified with nanosheets calcite at 300 ^{o}C. When it was calcite at higher temperature, the nanosheet on the surface of the hollow sphere transferred into nanoparticles. (Fig. S7) And when calcite at 500 ^{o}C, the Co_3O_4 shows nanorods morphology instead of nanosheet. It can be inferred that the nanosheet structure were transferred into nanorods at 500 ^{o}C.

3.3. Sensing performance

To investigate the sensing performance, the dynamic resistance curves for 300 second towards formaldehyde gas of Co_3O_4 calcite at 350 ^{o}C to 750 ^{o}C were obtained at room temperature (Fig. 8). It is clear that sensor's resistance decreases significantly when exposed to formaldehyde. The Co_3O_4 sensor calcite at 550 ^{o}C shows most prominent resistance decrease effect in 400 s. The sensing performance of Co_3O_4 nanosheet were also studied, the sensor fabricated by Co_3O_4 nanosheets also shows resistance decrease effect when exposed to formaldehyde.

Then, the sensing performance of the best Co_3O_4 sensors towards different concentration of formaldehyde vapors were studied. As shown in Fig. 10, the h-Co_3O_4-550 ^{o}C (Fig. 10A) and s-Co_3O_4-300 ^{o}C (Fig. 10B) sensor shows performance towards formaldehyde gas vapor at the concentration of 1 ppm, 5 ppm, 10 ppm, 50 ppm and 100 ppm. And the sensing response faster towards a higher concentration of formaldehyde. For the same exposure time for

formaldehyde, the resistance change is much higher at high formaldehyde concentration. The response value (R_g/R_a) of h-Co_3O_4-550 ^oC sensor can reach 17 after exposed to 100 ppm CH_2O gas vapor for 300 s. And the response value of s-Co_3O_4-300 ^oC can reach 35 in 18 s after exposed to 100 ppm CH_2O gas vapor. The h-Co_3O_4-550 ^oC sensor shows response value of 2.1 in 18 s at the same time. It shows that the s-Co_3O_4 shows better response towards CH_2O than h-Co_3O_4 at room temperature.

Dynamic sensing test were also studied on both Co_3O_4 hollow spheres and nanosheets. (Fig. S8 in supporting information). For the sensor's resistance cannot recover in a short time, each time after the sensor were exposed to formaldehyde gas vapor, a heating pulse at 200 ^oC for 30 seconds were performed to accelerate the desorption of formaldehyde molecules.

The selectivity towards various kinds of gas vapor were shown in Fig. 11. The sensing response were collected for exposure of the sensor for 10 seconds in 100 ppm gas vapors. The Co_3O_4 shows no response towards H_2, CO, CH_4, acetone, NH_3. And the sensor response value towards formaldehyde in 10 second are 4 and 20, respectively.

3.4. Sensing mechanism

Usually, the sensing response towards aldehyde were based on the oxidation of formaldehyde molecules, and the sensing temperature is mostly set at about 200 ^oC to help accelerate the oxidation reaction. At room temperature, gases are prone to be just adsorb on the nanomaterial and the oxidation effect is much

less prominent. In our previous work, we find the sensing behavior based on the electron transfer between amine molecules and In_2O_3 at room temperature. [33]

In this work, we study the Co_3O_4 response behavior at room temperature. We hypothesis it was induced by the adsorption effect and perform simulation of the adsorption behavior applying the VASP package. {110} plane of Co_3O_4 have been used to study the surface properties of cubic Co_3O_4. [34, 35] Formaldehyde molecules behavior that absorbed on the (110) plane of Co_3O_4 were optimized. The absorption energy (E_{ads}) was calculated according to the formula:

$$\triangle E_{ads}=E_{ads}-E_{surf}-E_{gas}$$

The adsorption energy was -2.83 eV. The negative adsorption energy means that the absorption behavior being exothermal process and the system is stable. [36] The density of states analysis can tell the electronic conductivity properties. It can be seen from Fig. that the density of states of Co_3O_4 at valance band as well as conduction band is elevated after CH_2O were simulated absorbed on the surface of the {110} plane of Co_3O_4. And the aldehyde molecules show density of state at the adsorption of formaldehyde has its HOMO energy close to the top of VB, then the electron can more easily move to the VB of Co_3O_4. [34] And the resistance of Co_3O_4 is elevated since that the amount of hole carrier is reduced. [22] It can be found that the adsorption of formaldehyde will the density state of Co_3O_4 nanomaterial on the nearby of conduction band. And the XPS data (Fig. S3 and S4) shows that the O 1s

spectra of h-Co_3O_4-550 has the composition of the active oxygen species at 532 eV. The active oxygen species help formaldehyde absorption.

The surface area shows enhanced sensing behavior towards formaldehyde vapor. The Co_3O_4 hollow spheres calcite at 550 ^oC exhibit the highest surface area. (9.8 m^2/g) And the N_2 absorption isothermal spectra (Fig. S5) also shows that h-Co_3O_4-550 has the highest surface area. And the sensor shows better sensing performance towards the same concentration of formaldehyde.

And the nanosheet structure also shows enhancement for the sensing performance. That Co_3O_4 nanosheet calcite at 300 ^oC exhibit the best sensing performance, which is consistence with the structure get from SEM as well as TEM.

Conclusion

In summary, we report aldehyde sensing performance at room temperature based on Co_3O_4 hollow spheres with different nanostructures. Both Co_3O_4 hollow spheres and nanosheets modified Co_3O_4 hollow spheres show response towards aldehyde at room temperature. And the response performance of nanosheets towards formaldehyde is much better than the nanoparticle construct Co_3O_4 hollow spheres. The surface oxygen species can enhance the sensing performance. And the Co_3O_4 hollow spheres shows nearly no response towards other common gas like CO, NH_3, acetone, etc.

4. Acknowledgement

Yang Cao and Yong Yang write the manuscript and do the experiment work. Jingyu Qian do the theoretical simulation work. Yong Yang and Yongguang Tu revised the manuscript.

5. Reference

[1] T. Salthammer, Formaldehyde in the ambient atmosphere: from an indoor pollutant to an outdoor pollutant? Angew. Chem. Int. Ed., 52(2013) 3320-3327.

[2] J. Flueckiger, F. K. Ko and K. C. Cheung, Microfabricated formaldehyde gas sensors, Sensors, 9(2009), 9196-9215.

[3] J. Zhang, J. L. Paul, and Q. He, Characteristics of aldehydes: concentrations, sources, and exposures for indoor and outdoor residential microenvironments, Environ. Sci. Technol., 28(1994), 146-152.

[4] R. Yang, K. Li. F. Liu, N. Li, F. Zhao and W. Chan, 3,3',5,5'-Tetramethyl-N-(9-anthrylmethyl)benzidine: A Dual-Signaling Fluorescent Reagent for Optical Sensing of Aliphatic Aldehydes, Anal. Chem., 75(2003), 3908-3914.

[5] Y. Suzuki, N. Nahano and K. Suzuki, Portable Sick House Syndrome Gas Monitoring System Based on Novel Colorimetric Reagents for the Highly Selective and Sensitive Detection of Formaldehyde, Environ. Sci. Technol., 37(2003), 5695-5700.

[6] A. Yasuhara and T. Shibamoto, Gas chromatographic determination of trace amounts of aldehydes in automobile exhaust by a cysteamine derivatization methods, J. Chromatogr. A, 672(1994) 261-266.

[7] K. Masunaga, K. Hayama, T. Onodera, K. Hayashi, N. Miura, K. Matsumoto and K. Toko, Polyacrylic acid polymer and aldehydes template molecule based MIPs coated QCM sensors for detection of pattern aldehydes in body odor, Sens. Actuators, B, 206(2015), 471-487.

[8] P. R. Chung, C. T. Tzeng, M. T. Ke and C. Y. Lee, Formaldehyde gas sensors: a review, Sensors, 13(2013), 4468-4484.

[9] S. Tian, X. Ding, D. Zeng, S. Zhang and C. Xie, Pore-size-dependent sensing property of hierarchical SnO_2 mesoporous microfibers as formaldehyde sensors, Sens. Actuators, B, 186(2013), 640-647.

[10] D. Calestani, R. Mosca, M. Zanichelli, M. Villani and A. Zappettini, Aldehyde detection by ZnO tetrapod-based gas sensors, J. Mater. Chem., 21(2011), 15532-15536.

[11] S. Lin, D. Li, J. Wu, X. Li and S. A. Akbar, A selective room temperature formaldehyde gas sensor using TiO_2 nanotube arrays, Sens. Actuators, B, 156(2011), 505-509.

[12] X. Wang, Y. Meng, G. D. Li, Y. Zou, Y. Cao and X. Zou, UV-assisted, template-free synthesis of ultrathin nanosheet-assembled hollow indium oxide microstructures for effective gaseous formaldehyde detection, Sens. Actuators, B, 224(2016), 559-567.

[13] L. Deng, X. Ding, D. Zeng, S. Tian, H. Li and C. Xie, Visible-light activate mesoporous WO_3 sensors with enhanced formaldehyde-sensing property at room temperature, Sens. Actuators, B, 163(2012), 260-266.

[14] A. Gurlo, Nanosensors: towards morphological control of gas sensing activity. SnO_2, In_2O_3, ZnO and WO_3 case studies, Nanoscale, 3(2011), 154-165.

[15] J. H. Lee, Gas sensors using hierarchical and hollow oxide nanostructures: overview, Sens. Actuators, B, 140(2009), 319-336.

[16] H. Yamamoto, S. Tanaka, T. Naito and H. Kazuyuki, Nonlinear change of refractive index of Co_3O_4 thin films induced by semiconductor laser (lambda= 405 nm) irradiation, Appl. Phys. Lett., 81(2002), 999-1001.

[17] Y. Liang, Y. Li, H. Wang, J. Zhou, J. Wang, T. Regier and H. Dai, Co_3O_4 nanocrystals on graphene as a synergistic catalyst for oxygen reduction reaction, Nat. Mater., 10(2011), 780-786.

[18] L. Hu, Q. Peng and Y. Li, Selective synthesis of Co_3O_4 nanocrystal with different shape and crystal plane effect on catalytic property for methane combustion, J. Am. Chem. Soc., 130(2008), 16136-16137.

[19] H. J. Qiu, L. Liu, Y. P. Mu, H. J. Zhang and Y. Wang, Designed synthesis of cobalt-oxide-based nanomaterials for superior electrochemical energy storage devices, Nano Res., 8(2015), 321-339.

[20] A. J. Esswein, Size-dependent activity of Co_3O_4 nanoparticle anodes for alkaline water electrolysis, J. Phys. Chem. C, 113(2009), 15068-15072.

[21] J. M. Xu and J. P. Cheng, The advances of Co_3O_4 as gas sensing materials: A review, J. Alloy. Compd., 686(2016), 753-768.

[22] H. J. Kim and J. H. Lee, Highly sensitive and selective gas sensors using p-type oxide semiconductors: overview, Sens. Actuators, B, 192(2014), 607-627.

[23] C. Sun, X. Su, F. Xiao, C. Niu and J. Wang, Synthesis of nearly monodisperse Co_3O_4 nanocubes via a microwave-assisted solvothermal process and their gas sensing properties, Sens. Actuators, B, 157(2011), 681-685.

[24] J. Deng, R. Zhang, L. Wang, Z. Lou and T. Zhang, Enhanced sensing performance of the Co_3O_4 hierarchical nanorods to NH_3 gas, Sens. Actuators, B, 209(2015), 449-455.

[25] T. Akamatsu, T. Itoh, N. Izu and W. Shin, NO and NO_2 sensing properties of WO_3 and Co_3O_4 based gas sensors, Sensors, 13(2013), 12467-12481.

[26] S. Vetter, S. Haffer, T. Wagner and M. Tiemann, Nanostructured Co_3O_4 as a CO gas sensor: temperature-dependent behavior, Sens. Actuators, B, 206(2015), 133-138.

[27] J. Y. Kim, N. J. Choi, H. J. Park, J. Kim, D. S. Lee, and H. Song, A hollow assembly and its three-dimensional network formation of single-crystalline Co_3O_4 nanoparticles for ultrasensitive formaldehyde gas sensors, J. Phys. Chem. C, 118(2014), 25994-26002.

[28] Y. Liu, G. Zhu, B. Ge, H. Zhou, A. Yuan and X. Shen, Concave Co_3O_4 octahedral mesocrystal: polymer-mediated synthesis and sensing properties, CrystEngComm, 14(2012), 6264-6270.

[29] S. Wang, C. X, P. Wang, Z. Li, B. Xiao, R. Zhao, T. Yang and M. Zhang, Mater. Lett., 137(2014), 289-292.

[30] C. Q. Lv, C. Liu and G. C. Wang, A DFT study of methanol oxidation on Co_3O_4, Catal. Commun., 45(2014), 83-90.

[31] J. Zhao, Y. Zou, X. Zou, T. Bai, Y. Liu, R. Gao, D. Wang and G. D. Li, Self-template construction of hollow Co_3O_4 microspheres from porous ultrathin nanosheets and efficient noble metal-free water oxidation catalysts, Nanoscale, 6(2014), 7255-7262.

[32] G. Kresse, J. Furthmüller, Phys. Rev. B, 54(1996), 11169-11186.

[33] G. Kresse, J. Furthmüller, Comp. Mater. Sci., 6(1996), 15-50.

[34] Y. Cao, X. Huang, Y. Wu, Y. Zou, J. Zhao, G. D. Li and X. Zou, Three-dimensional ultrathin In_2O_3 nanosheets with morphology-enhanced activity for amine sensing, RSC Adv., 5(2015), 60541-60548.

[35] X. L. Xu, E. Yang, J. Q. Li, Y. Li and W. K. Chen, A DFT Study of CO Catalytic Oxidation by N_2O or O_2 on the Co_3O_4 (110) Surface, ChemCatChem, 1(2009), 384-392.

[36] X. Y. Pang, C. Liu, D. C. Li, C. Q. Lv and G. C. Wang, Structure Sensitivity of CO Oxidation on Co_3O_4: A DFT Study, ChemPhysChem, 14(2013), 204-212.

[37] W. Zeng, T. M. Liu and D. J. Liu, Formaldehyde gas sensing property and mechanism of TiO_2-Ag nanocomposite, Physica B, 405(2010), 4235-4239.

Figure captions:

Fig. 1 Scheme for synthesis for Co_3O_4 hollow spheres.

Fig. 2 Scheme for synthesis for Co_3O_4 nanosheets.

Fig. 3 (A) SEM and TEM (B) XRD for the cobalt glycerolate.

Fig. 4 XRD for h-Co_3O_4 (Co_3O_4 hollow spheres) calcite at 350 ^oC-750 ^oC.

Fig. 5 SEM for h-Co_3O_4 calcite at (A)350 ^oC, (B)450 ^oC, (C)550 ^oC, (D)650 ^oC, (E) 750 ^oC.

Fig. 6 TEM for h-Co_3O_4 hollow spheres calcite at 550 ^oC.

Fig. 7 XRD for s-Co_3O_4 (Co_3O_4 nanosheets) calcite from 300 ^oC to 500 ^oC.

Fig. 8 SEM and TEM for Co_3O_4 nanosheets.

Fig. 9 The sensing performance of (A) h-Co_3O_4 (Co_3O_4 hollow spheres) and (B) s-Co_3O_4 (Co_3O_4 nanosheets) towards 10 ppm aldehyde operate at room temperature.

Fig. 10 The sensing performance of (A) h-Co_3O_4 (Co_3O_4 hollow spheres) calcite at 550 ^oC) and (B) s-Co_3O_4 (Co_3O_4 nanosheets calcite at 300 ^oC) towards different concentration of aldehyde.

Fig. 11 The selectivity towards various kind of gas of 100 ppm after exposure for 10 sec.

Fig. 12 The DOS states of Co_3O_4 crystal before and after adsorption of aldehyde.

Figure1

Click here to download high resolution image

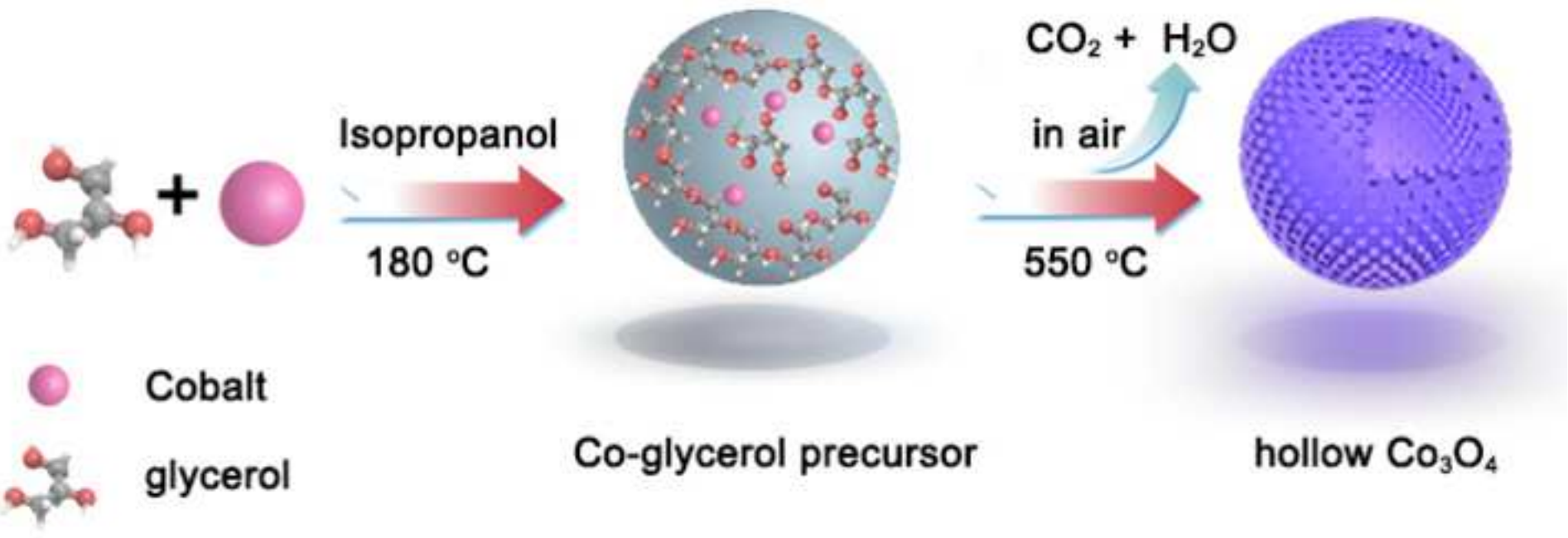

Figure2

https://doi.org/10.26434/chemrxiv.12436979.v1

ORCID: https://orcid.org/0000-0002-5251-8747

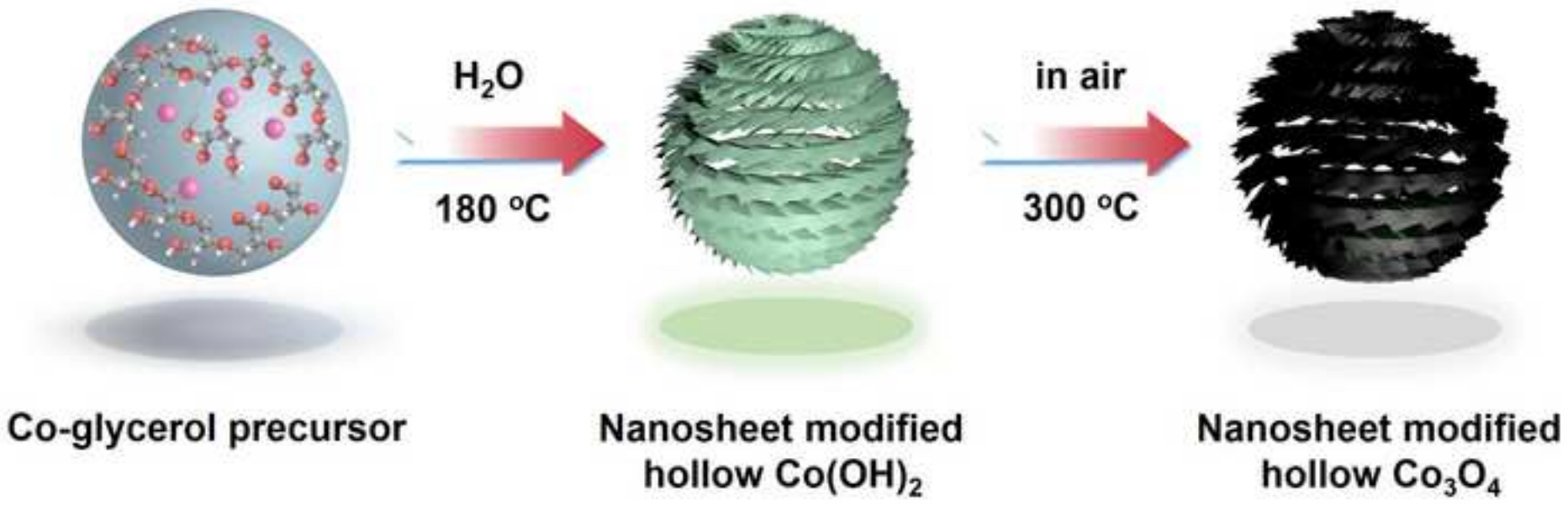

Figure3

Click here to download high resolution image

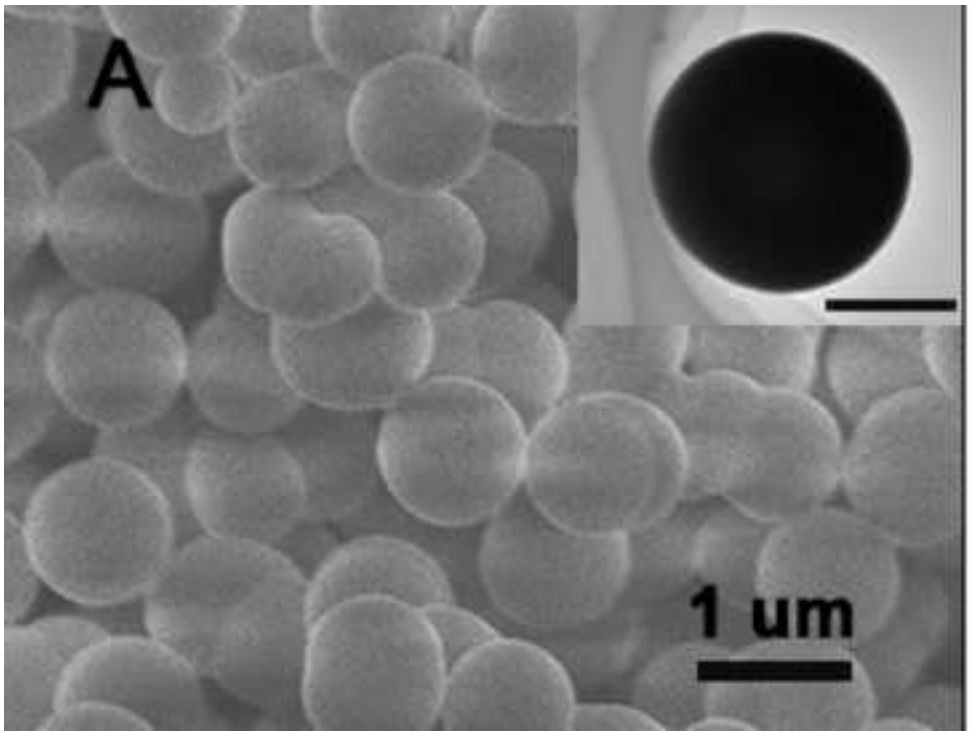

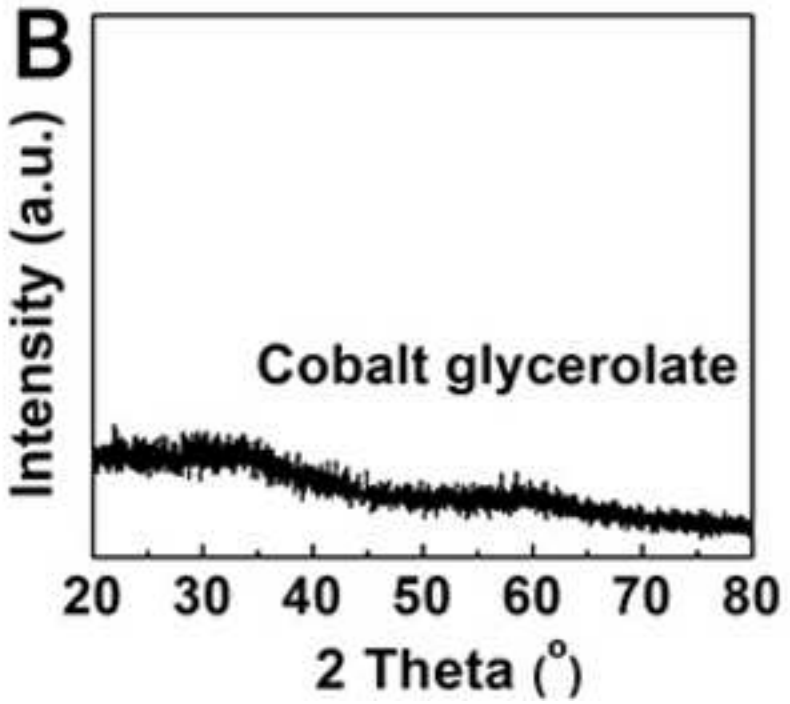

Figure4

Click here to download high resolution image

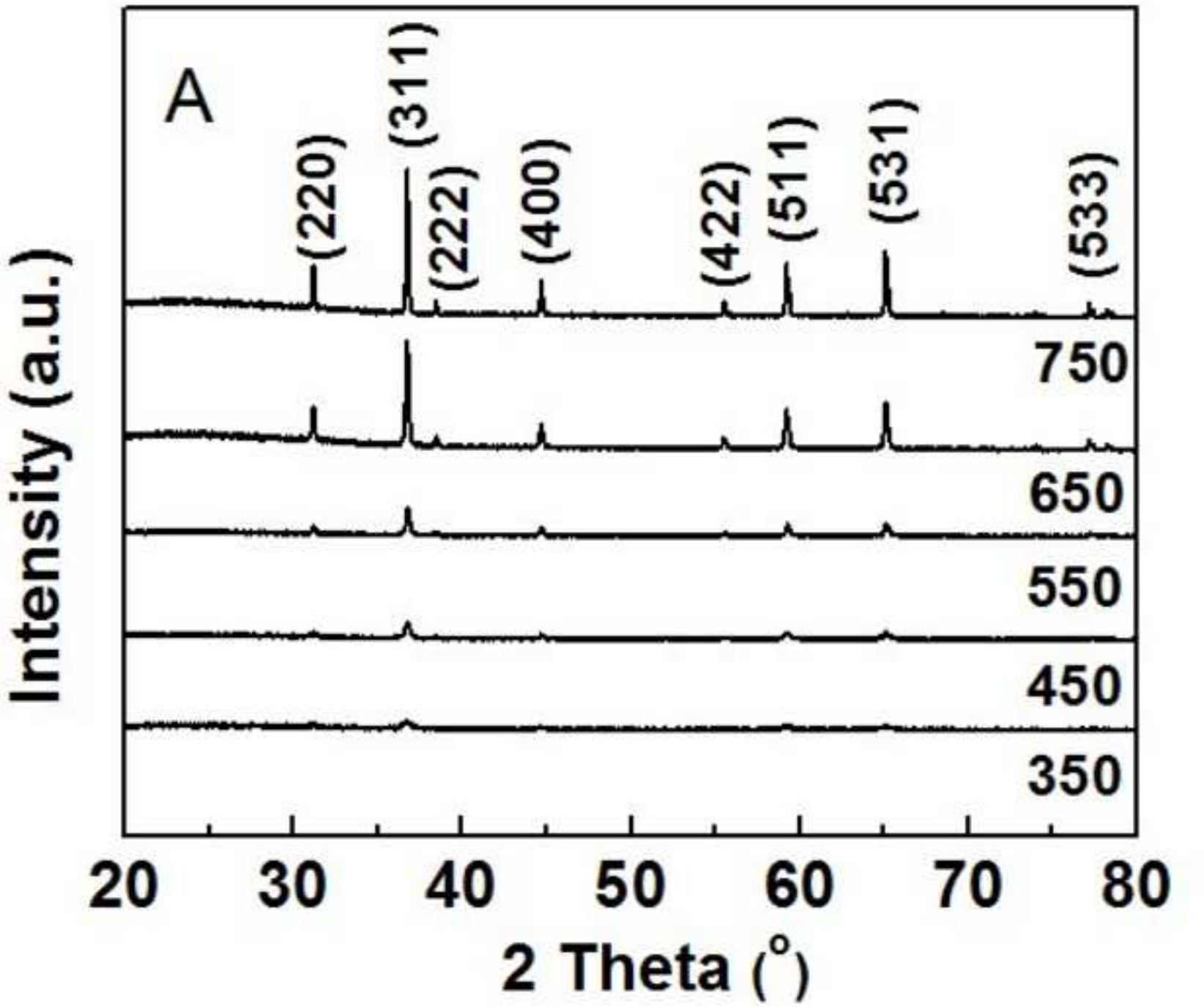

Figure5

Click here to download high resolution image

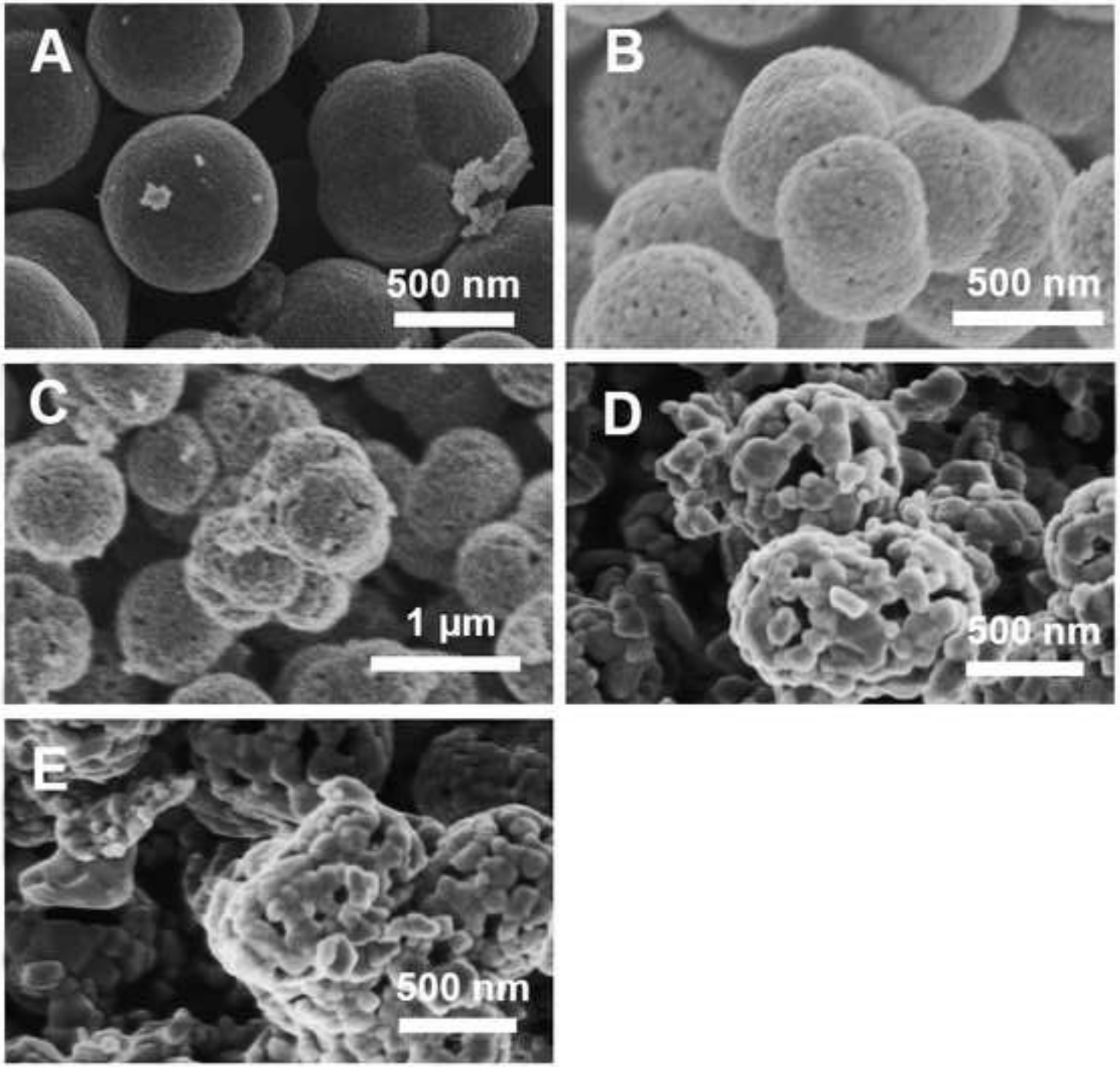

Figure6

Click here to download high resolution image

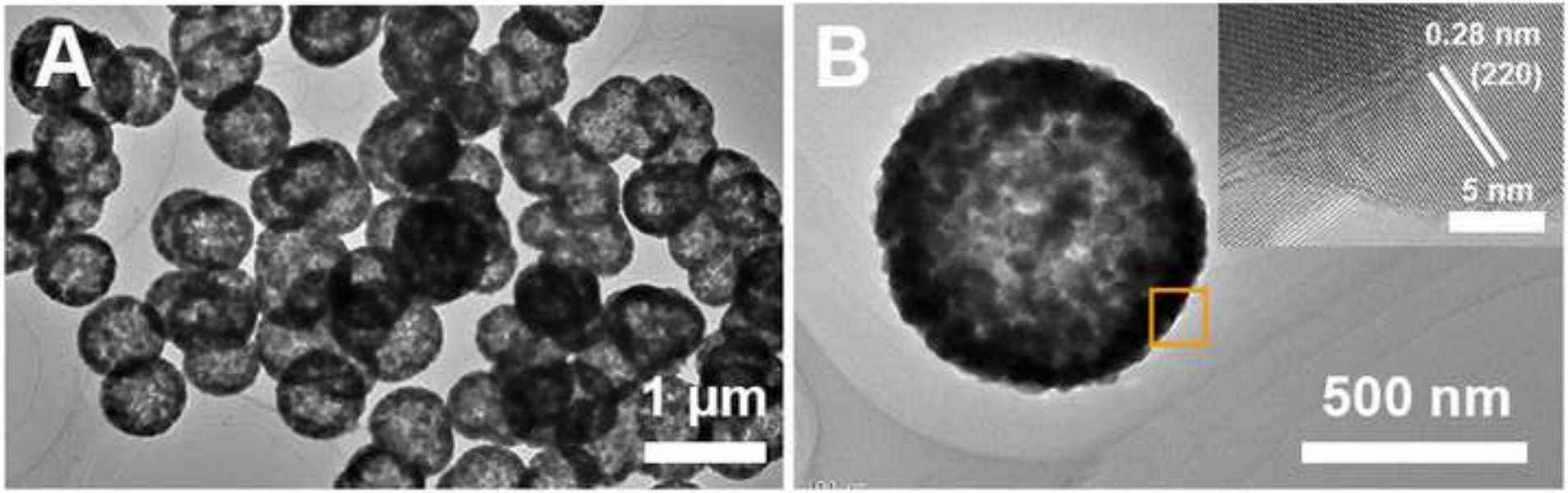

Figure7

Click here to download high resolution image

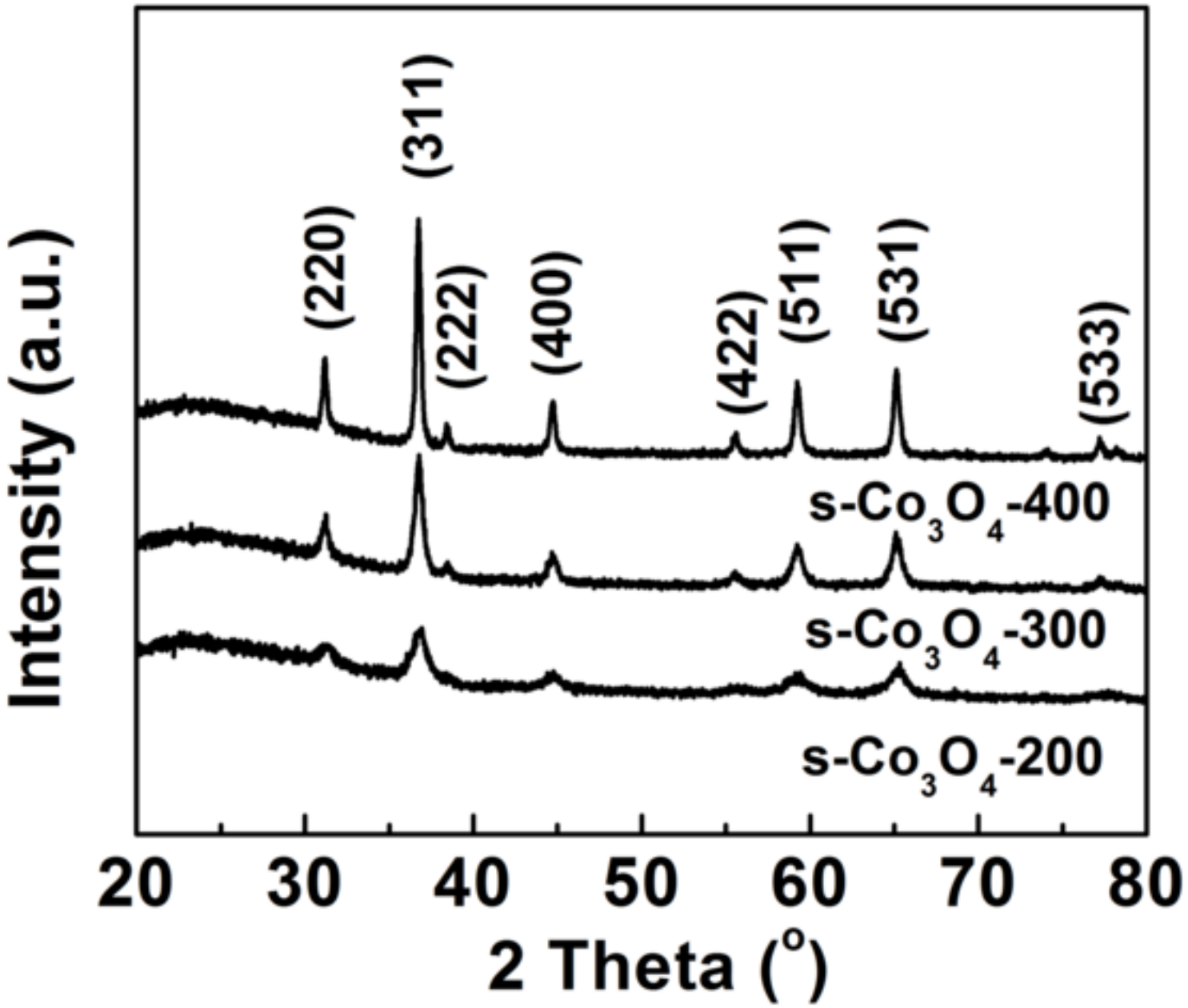

Figure8

Click here to download high resolution image

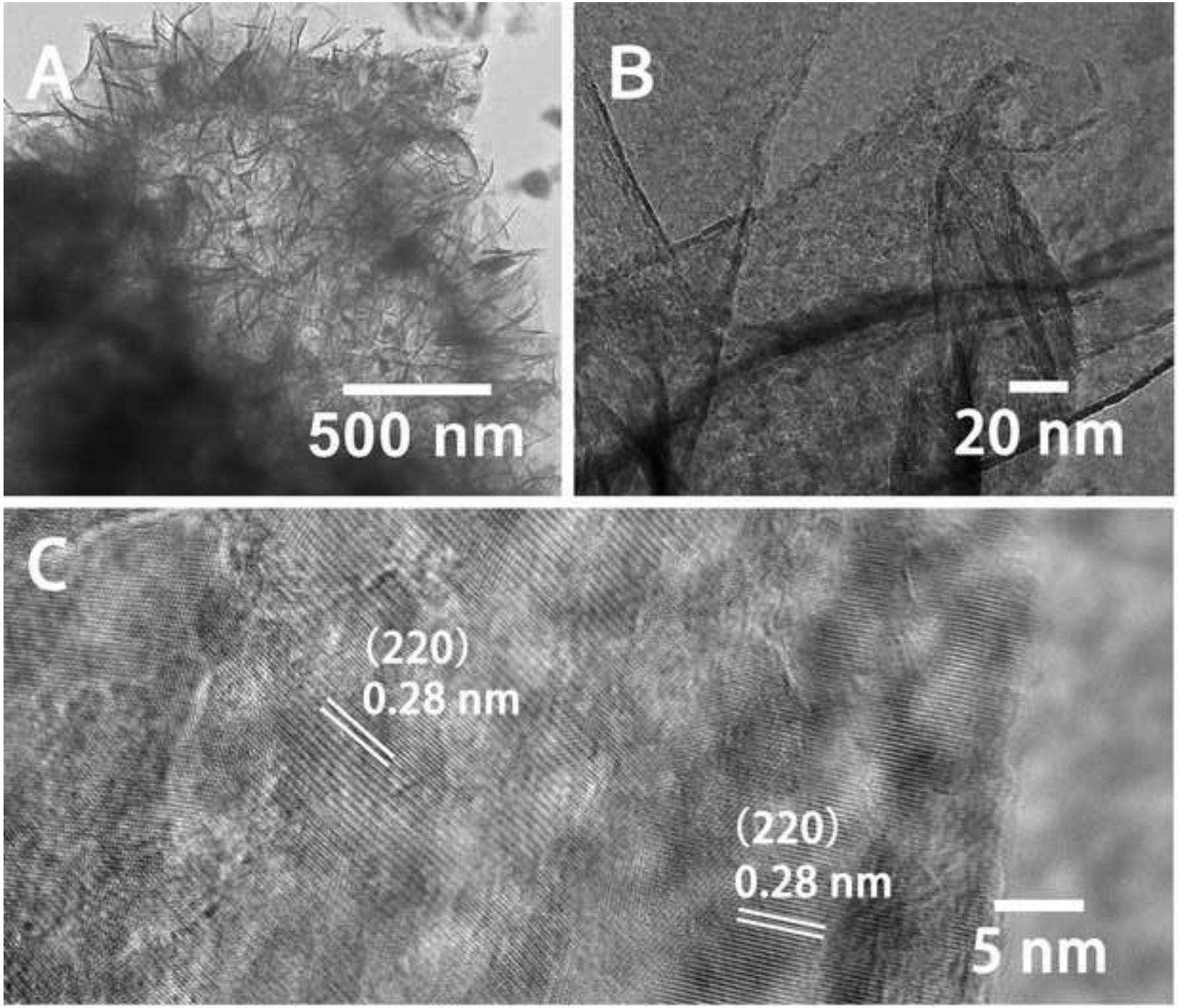

Figure9

Click here to download high resolution image

https://doi.org/10.26434/chemrxiv.12436979.v1 ORCID: https://orcid.org/0000-0002-5251-8747

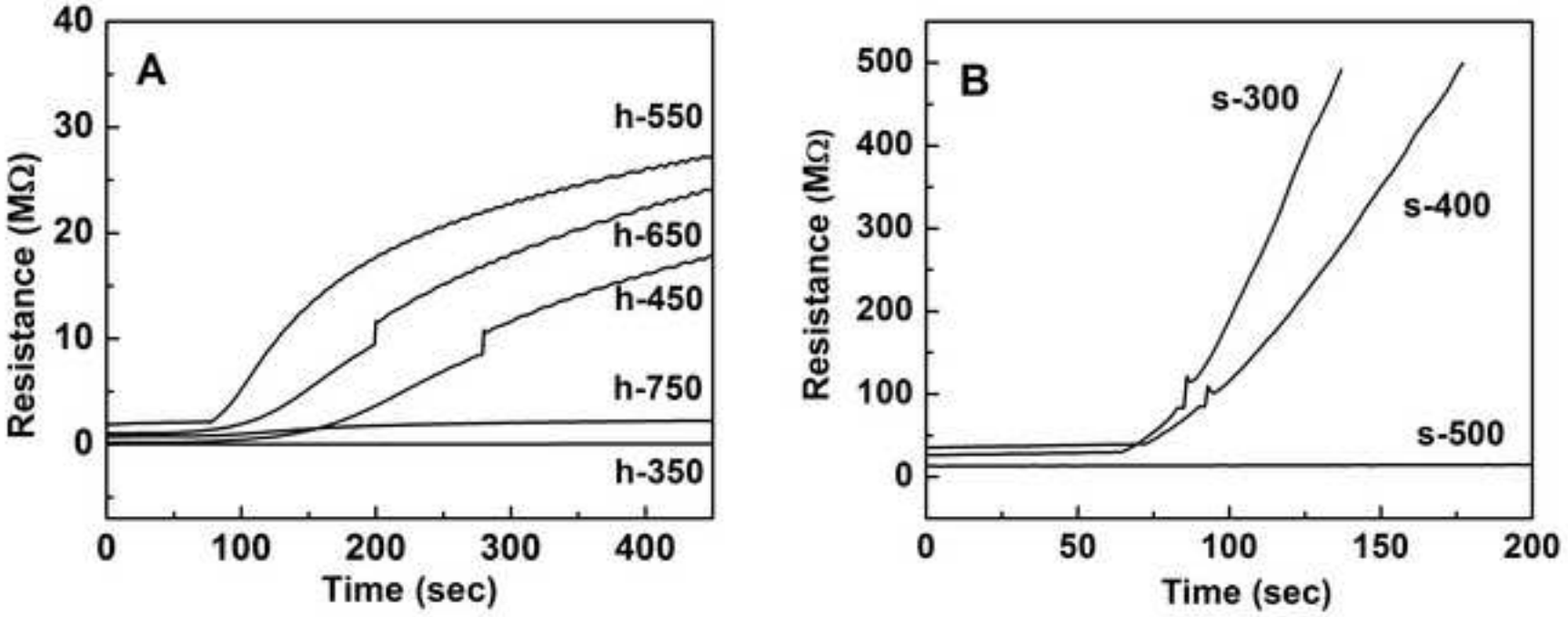

Figure10

Click here to download high resolution image

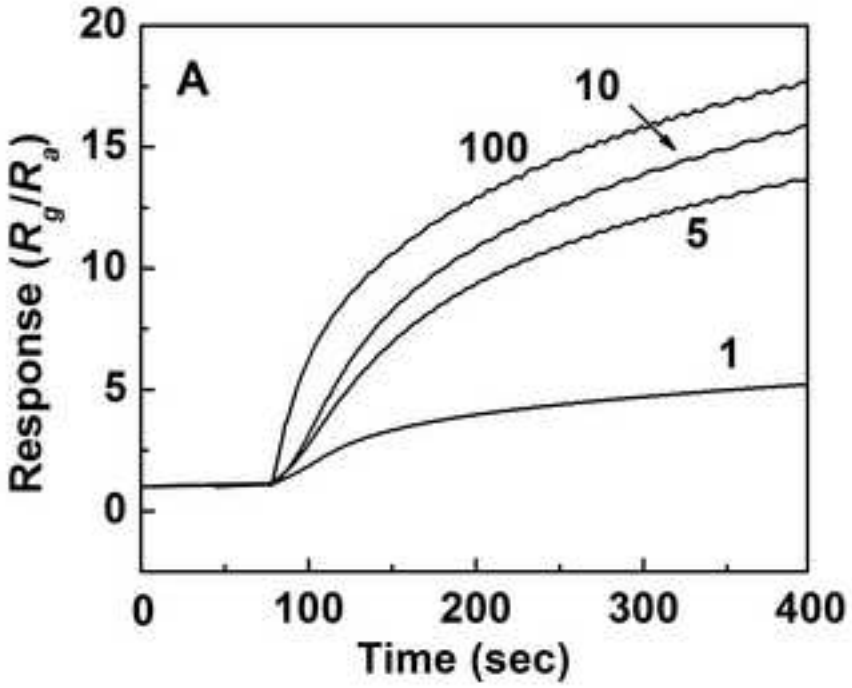

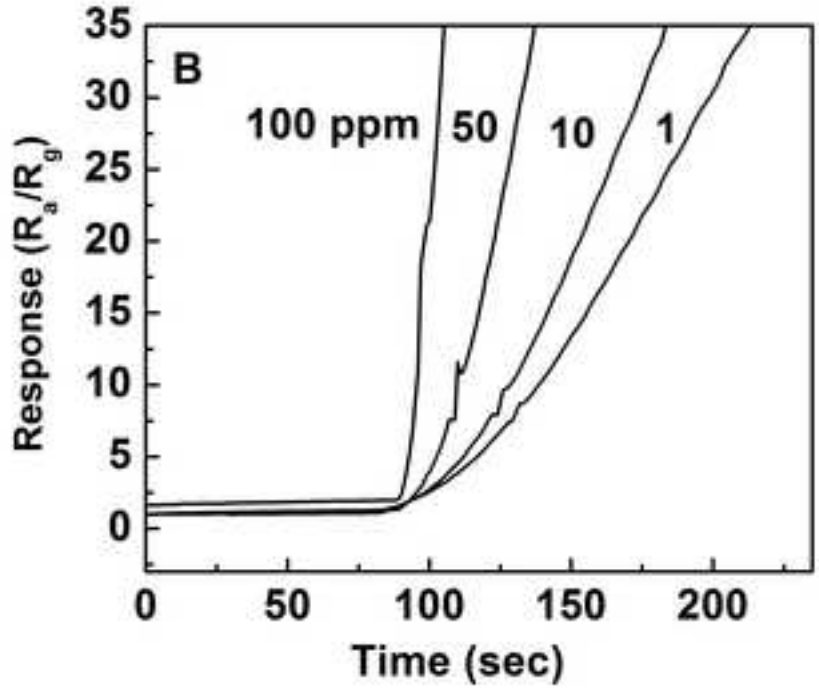

Figure11

Click here to download high resolution image

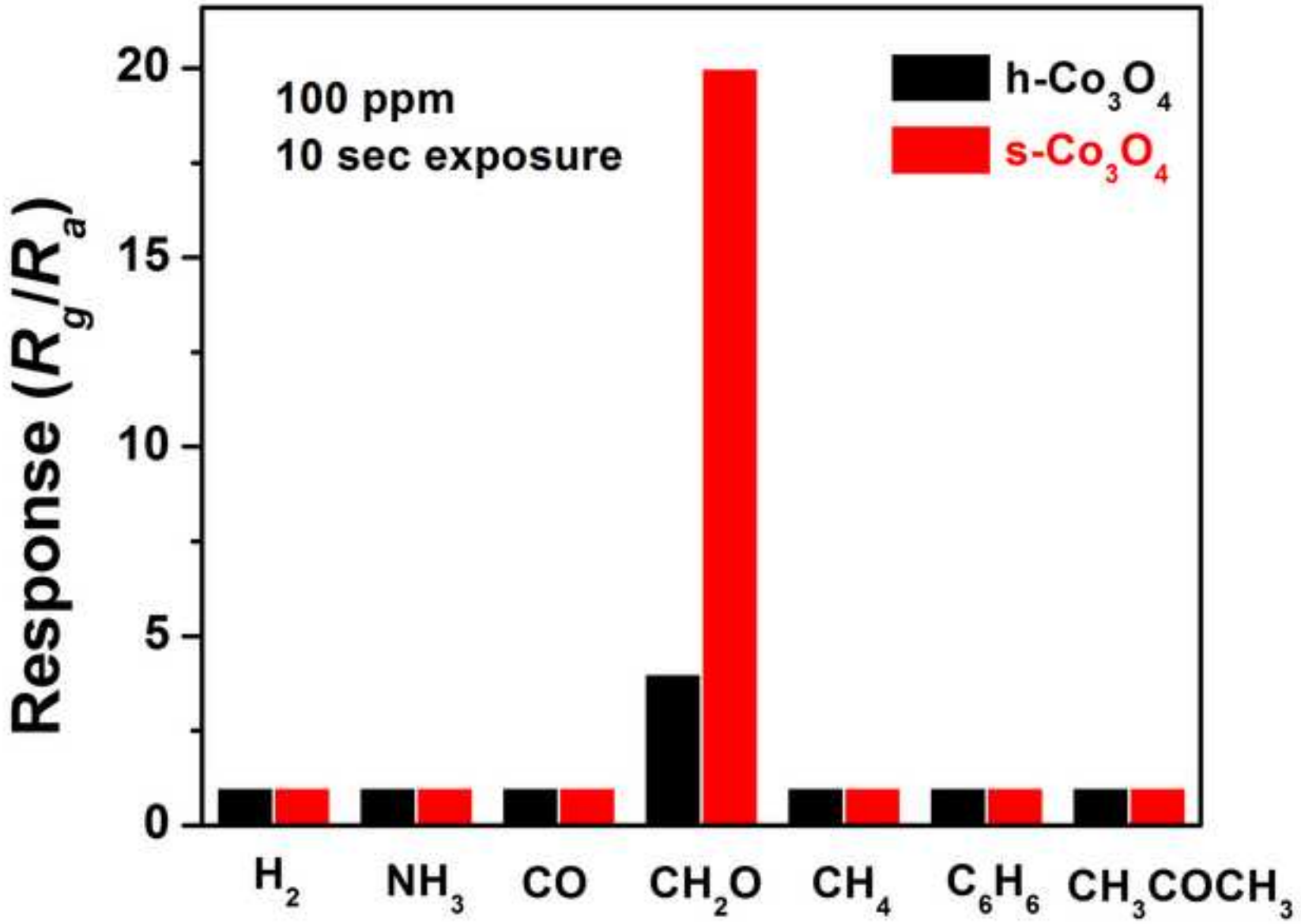

Figure12

Click here to download high resolution image

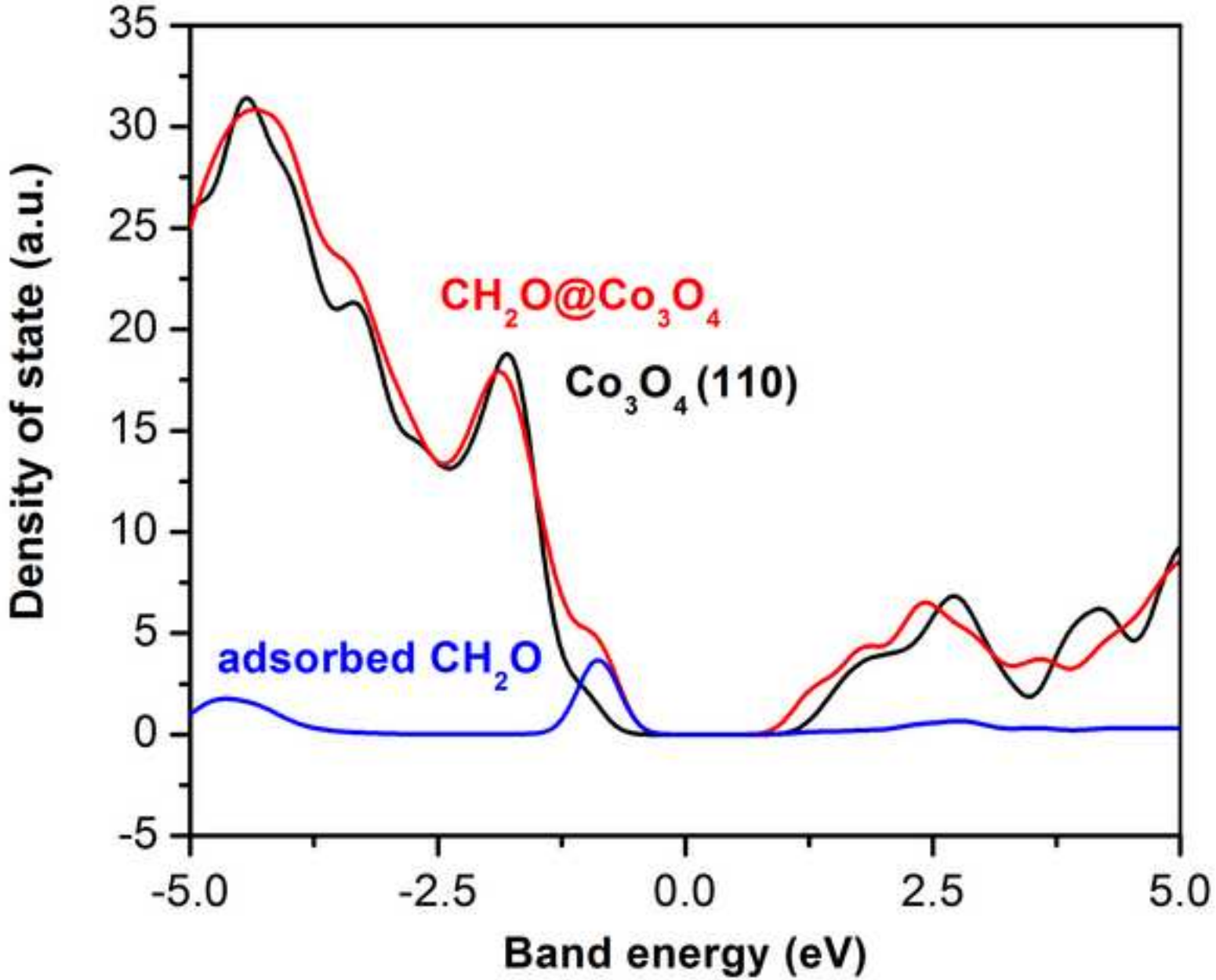

Supplementary Material

Click here to download Supplementary Material: Supplementary Material.docx

Research Highlights：

1. Room temperature sensing of formaldehyde by fabricate of Co_3O_4 nanostructures.
2. Selective response towards aldehyde gas, while not response towards NH_3, CO, etc.
3. The relationship between the nanostructure and the sensing performance.

Electronic Supplementary Information (ESI):

Formaldehyde sensing by Co_3O_4 hollow spheres at room temperature

Yang Cao [a*], Jingyu Qian[b], Yong Yang [c], Yongguang Tu [d]

a Department of Energy and Resources Engineering, College of Engineering, Peking University, Beijing, 100871 PR China

b State Key Laboratory of Supramolecular Structure and Materials, College of Chemistry, Jilin University, 2699 Qianjin Street, Changchun 130012, China

c State Key Laboratory of Solidification Processing Center of Advanced Lubrication and Seal Materials, Northwestern Polytechnical University, Xi'an, Shaanxi 710072, P. R. China

d State Key Laboratory for Artificial Microstructure and Mesoscopic Physics, Department of Physics, Peking University, Beijing 100871, China.

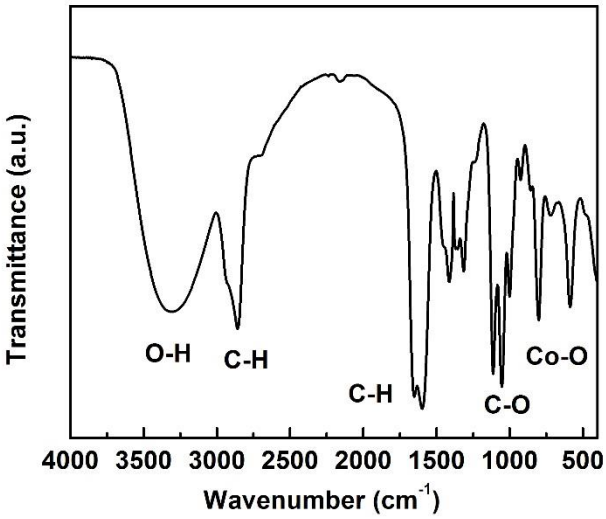

Fig. S1. The FT-IR spectra of cobalt glycerolate.

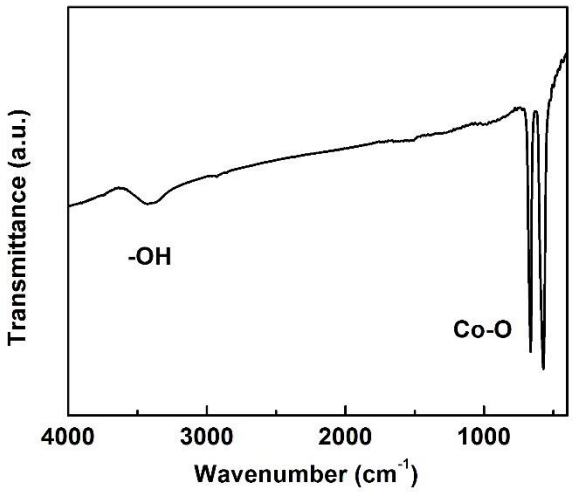

Fig. S2. Typical FT-IR spectra of hollow Co_3O_4. (h-Co_3O_4-550)

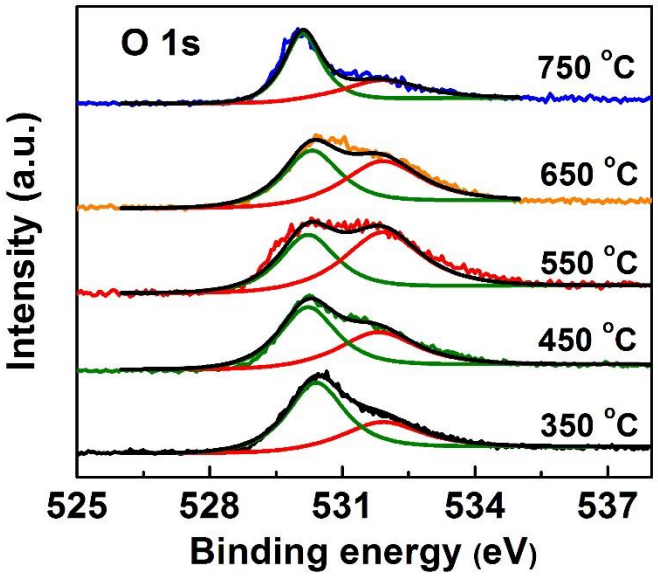

Fig. S3. O 1s XPS spectroscopy for h-Co_3O_4.

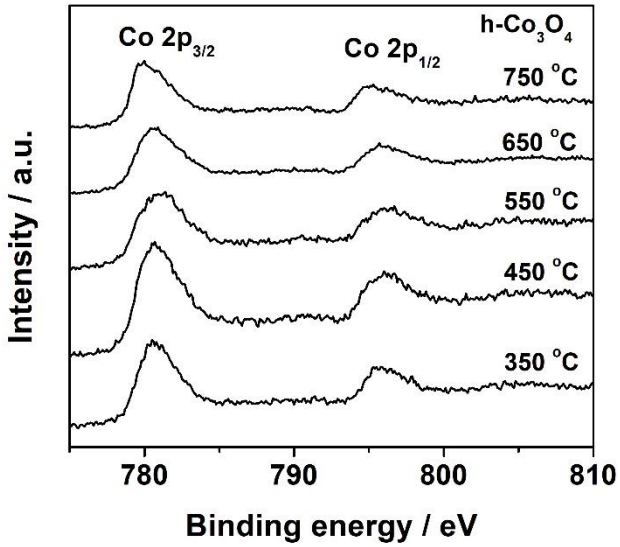

Fig. S4. Co 2p XPS spectroscopy for h-Co_3O_4.

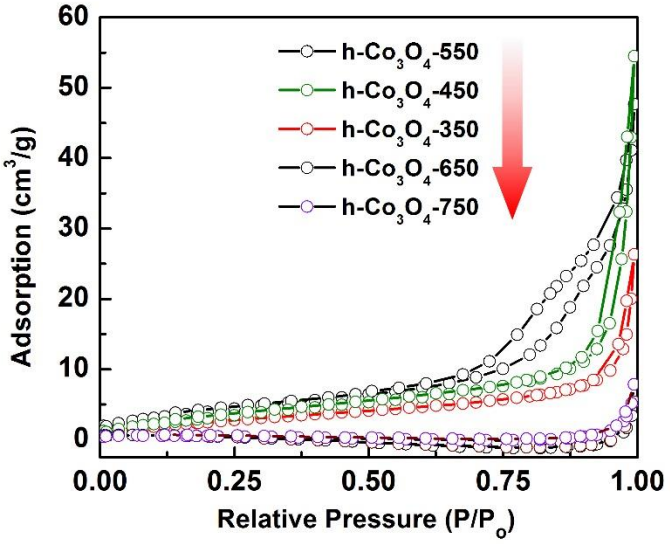

Fig. S5. N_2 absorption isotherm spectra for h-Co_3O_4.

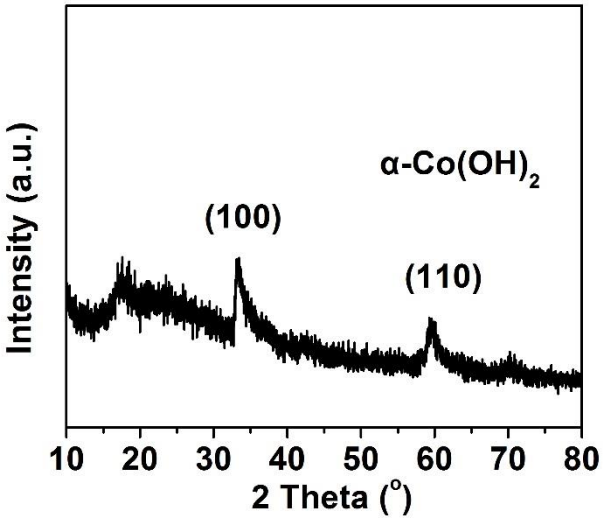

Fig. S6. XRD pattern for $Co(OH)_2$ nanosheet.

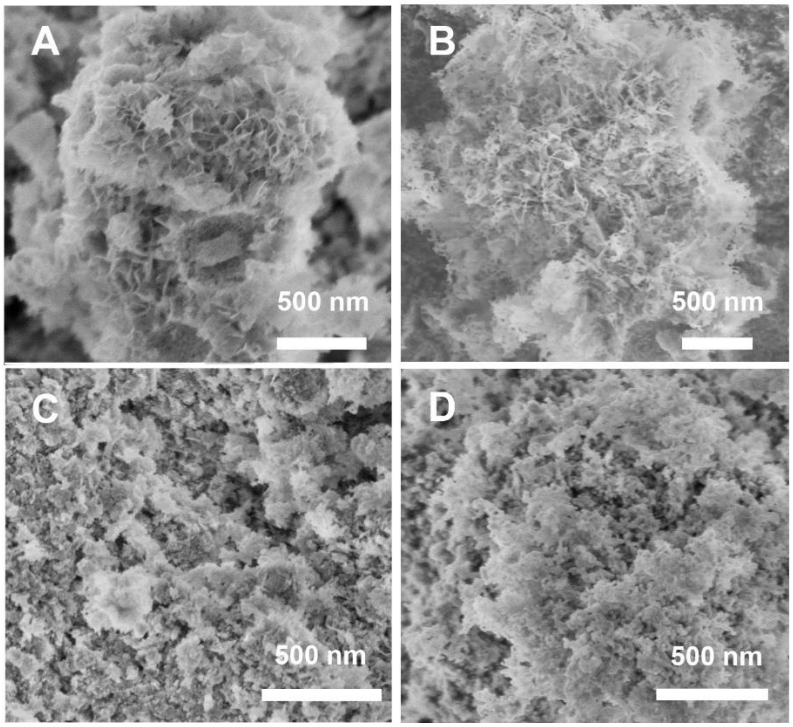

Fig. S7. SEM spectra for (A) $Co(OH)_2$ and Co_3O_4 calcite at (B) 300 ºC, (C) 400 ºC, (D) 500 ºC.

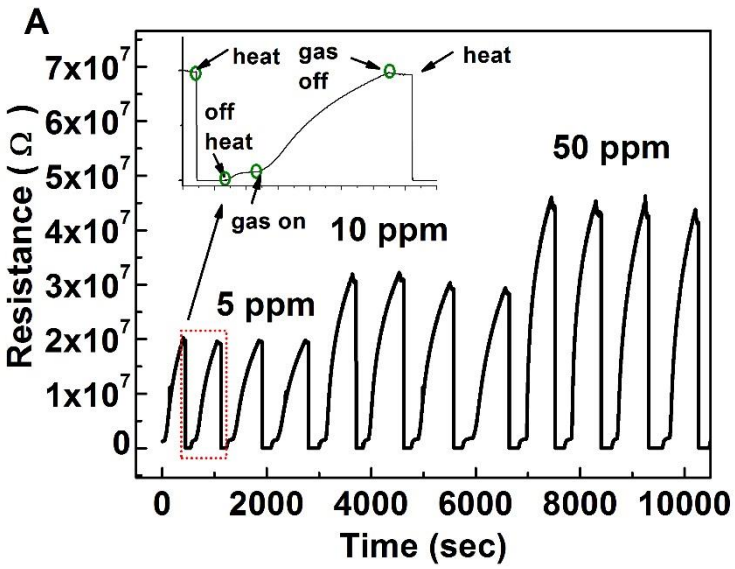

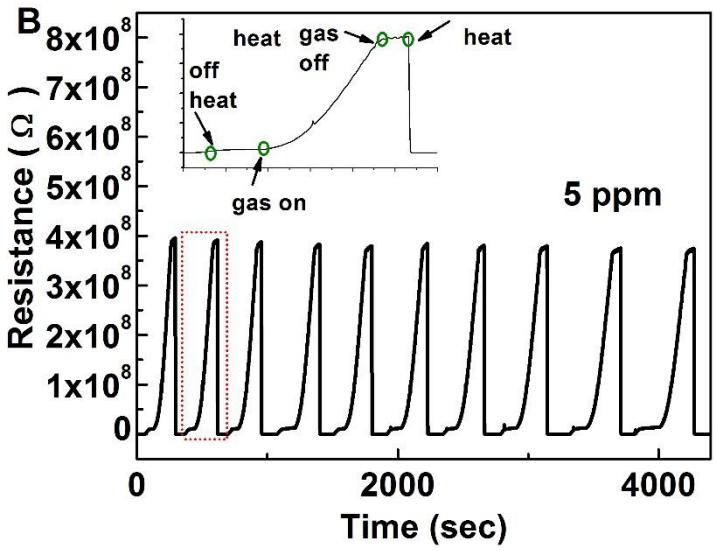

Fig. S8. Dynamic response curve of (A) h-Co_3O_4-550 and (B) s-Co_3O_4-300.